Extended x-ray absorption fine structure study of $MnFeP_{0.56}Si_{0.44}$ compound*

Li Ying-Jie(李英杰)[a], Haschaolu W(哈斯朝鲁)[a], Wurentuya(乌仁图雅)[a], Song Zhi-Qiang(宋志强)[a], Ou Zhi-Qiang(欧志强)[a], Tegus O(特古斯)[b]†, and Nakai Ikuo(中井生央)[b]

[a] *Inner Mongolia Key Laboratory for Physics and Chemistry of Functional Materials, Physics and Electronic Information College, Inner Mongolia Normal University, Hohhot* 010022, *China*

[b] *Department of Electrical and Electronic Engineering, Tottori University, Tottori* 680-8552, *Japan*

(Received 4 November 2014; revised manuscript received 31 March 2015; published online 20 June 2015)

The $MnFeP_{0.56}Si_{0.44}$ compound is investigated by x-ray diffraction, magnetic measurements, and x-ray absorption fine structure spectroscopy. It crystallizes in Fe_2P-type structure with the lattice parameters $a = b = 5.9823(0)$ Å and $c = 3.4551(1)$ Å and undergoes a first-order phase transition at the Curie temperature of 255 K. The Fe K edge and Mn K edge x-ray absorption fine structure spectra show that Mn atoms mainly reside at 3g sites, while 3f sites are occupied by Fe atoms. The distances between the absorbing Fe atom and the first and second nearest neighbor Fe atoms in a 3f-layer shift from 2.65 Å and 4.01 Å in the ferromagnetic state to 2.61 Å and 3.96 Å in the paramagnetic phase. On the other hand, the distance between the 3g-layer and 3f-layer changes a little as 2.66 Å–2.73 Å below the Curie temperature and 2.68 Å–2.75 Å above it.

Keywords: $MnFeP_{0.56}Si_{0.44}$ compound, Mn K edge, Fe K edge, EXAFS, local structure

PACS: 61.05.cj, 32.30.Rj **DOI:** 10.1088/1674-1056/24/8/086101

1. Introduction

Magnetic refrigeration based on the magnetocaloric effect has attracted much attention as an energy saving and environmentally friendly alternative to conventional gas-compression refrigeration.[1,2] In 1997, Pecharsky *et al.*[3,4] discovered a giant magnetocaloric effect in $Gd_5Si_2Ge_2$ in the vicinity of the first-order phase transition. A lot of magnetocaloric materials with the first-order phase transition have since been reported such as MnAs-based alloys,[5] $MnFeP_xAs_{1-x}$,[2] and $Mn_{1.1}Fe_{0.9}P_xGe_{1-x}$[6] compounds. Recently an Fe_2P-type $Fe_{2-x}Mn_x$(P, Si) compound has been intensively investigated as a promising candidate for room-temperature magnetic refrigeration.[7] The first-order phase transition usually relates to a structural deformation. In an Fe_2P-type compound, the lattice parameters a and c undergo a discontinuous change, while the volume hardly changes, either below or above the transition temperature.[8]

Zhang *et al.* showed that Mn and Fe atoms preferentially occupy the 3g and 3f sites in $FeMnP_{0.6}Si_{0.4}$, while P and Si are randomly distributed at the 1b and 2c sites.[9] Höglin *et al.* suggested that the Fe atoms are mainly situated in the 3g site, while the Mn atoms prefer the 3f position in $FeMnP_{0.5}Si_{0.5}$.[10] Their results conflict. To settle the controversy, we undertook an extended x-ray absorption fine structure (EXAFS) study of FeMn(P, Si). EXAFS is a powerful tool to probe the local atomic arrangements around a specific atom, such as coordination number and interatomic distance. In a previous study, we measured near Fe K edge EXAFS and reported on the local structure around Fe atoms for an Mn-rich $Mn_{1.28}Fe_{0.67}P_{0.46}Si_{0.54}$ compound.[11] Although it was only for the Fe K edge EXFAS, we found that the Mn atoms are located mainly at the 3g sites and that the 3f sites are occupied by Fe atoms and Mn atoms randomly. To get more understanding of the local structure of FeMn(P, Si), we carried out an EXAFS study on an $MnFeP_{0.56}Si_{0.44}$ compound. In the present work, we report on the local structure around both Fe and Mn atoms for $MnFeP_{0.56}Si_{0.44}$ and the interplay between the microscopic structure and the magnetic phase transition.

2. Experiment

A polycrystalline ingot of $MnFeP_{0.56}Si_{0.44}$ was synthesized by high-energy ball milling and a solid-state reaction. The proper amounts of Mn (99.9%), Si (99.99%), Fe (99.5%), and red-P (99.999%) were mixed and ball-milled for 72 hours in a vacuum. The fine powder was then pressed into a small pellet and sealed in a quartz ampoule in an Ar atmosphere of 200 mbar (1 bar = 10^5 Pa). It was sintered at 1150 °C for 2 hours, annealed at 850 °C for 20 hours and then cooled down to room temperature. The x-ray diffraction was measured using Cu Kα radiation in a conventional θ–2θ scan

*Project supported by the National Natural Science Foundation of China (Grant Nos. 51461035, 51161017, and 11404176), the Scientific Research Projects of the Higher Educational Department of Inner Mongolian Autonomous Region, China (Grant No. NJZZ14033). The XAFS measurement was performed under the approval of Photon Factory Program Advisory Committee (Proposal Nos. 2012G095 and 2014G047).

†Corresponding author. E-mail: tegusph@imnu.edu.cn

© 2015 Chinese Physical Society and IOP Publishing Ltd

mode. Magnetic measurements were carried out in a vibrating sample magnetometer (Lakeshore 7407 VSM) between 150 K and 300 K and in magnetic fields up to 0.5 T. The EXAFS measurements near Fe and Mn K edges were performed using synchrotron radiation at the beamline BL12C of Photon Factory.[12] The storage ring was operated in the top-up mode at 2.5 GeV with a beam current of about 450 mA. The Si (111) double crystal monochromator was installed in the optics system. All the spectra were measured at 25 K, 100 K, 200 K, and 295 K in the transmission mode with the intensities of incident and transmitted x-ray beams measured using the ionization chambers filled with pure N_2 gas in front of the sample and a mixed gas of 85% N_2 and 15% Ar behind the sample. The incident energy of photons was calibrated with the energy value for a peak near the Cu K edge. The sample was powdered and uniformly spread onto scotch tape. For EXAFS measurements we piled up several layers of tape to obtain an appropriate absorption. The full spectrum at the Mn and Fe K edges was accumulated at intervals of 0.3 eV near the edges and at 2.5-eV intervals in the EXAFS range.

3. Results and discussion

Figure 1 shows the x-ray diffraction pattern of $MnFeP_{0.56}Si_{0.44}$ at room temperature, which shows that the $MnFeP_{0.56}Si_{0.44}$ compound crystallizes in a single phase of the hexagonal structure with $P\bar{6}2m$ space group. The Rietveld refinement gives the lattice parameters $a = b = 5.9823(0)$ Å and $c = 3.4551(1)$ Å with the R-factors of 9.24%. As shown in Fig. 2, the Mn/Fe atoms, denoted by large spheres, form a triangle, with the first and second nearest neighbor atoms at the 3f-layer and the first nearest neighbor atoms at the 3g-layer, while P and Si atoms are randomly distributed at the 1b and 2c sites. The single P/Si (1b) atom and four P/Si (2c) atoms, denoted by small spheres, form a conical structure; the two P/Si (1b) atoms and two P/Si (2c) atoms form a tetrahedral structure. The P/Si (1b, 2c) atoms are stacked alternately in 3f and 3g layers. All the phosphides, such as Fe_2P and Mn_2P, possess the same structure.

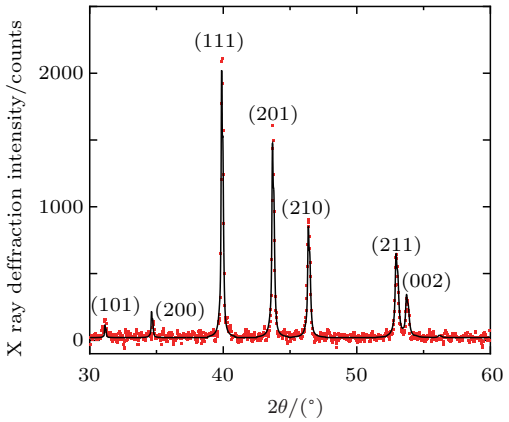


Fig. 1. (color online) X-ray powder diffraction patterns of $MnFeP_{0.56}Si_{0.44}$ taken at 295 K. The typical indices of the reflections are labeled.

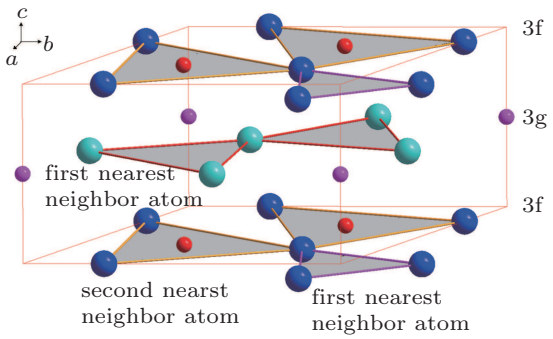


Fig. 2. (color online) Local atomic configuration of $MnFeP_{0.56}Si_{0.44}$ around the 3g site and the 3f site denoted by large spheres (Fe/Mn) and small ones (P/Si). The triangles composed of the 3g sites and the 3f sites are stacked alternately along the c-plane.

Figure 3 shows the temperature dependence of the magnetization of $MnFeP_{0.56}Si_{0.44}$, measured in a magnetic field of 0.05 T, with increasing temperature followed by decreasing temperature. The thermal hysteresis between the warming and cooling curves indicates that the magnetic transition between the paramagnetic and ferromagnetic phases is of the first order. The Curie temperature (in the warming process) is 255 K, which is determined by the temperature, where the first derivative of the magnetization on temperature, shows its extreme value.

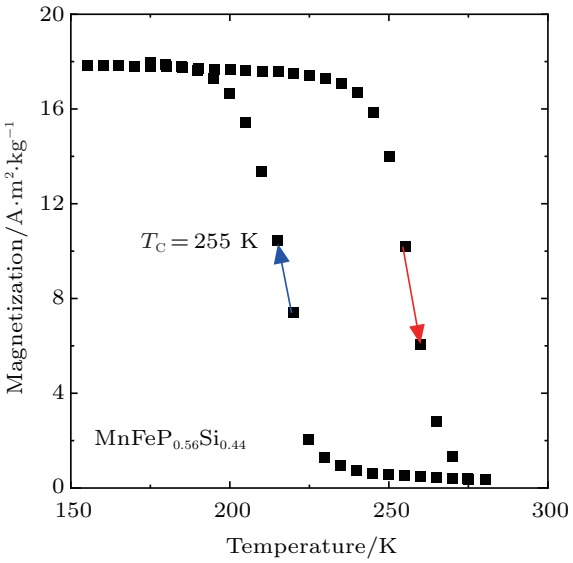


Fig. 3. (color online) Temperature dependence of the magnetization of $MnFeP_{0.56}Si_{0.44}$, measured in a field of 0.05 T with increasing temperature and decreasing temperature, where T_C is the phase transition temperature in the warming process.

The total x-ray absorption $\mu_{ob}(E)$ as a function of incident photon energy E is given as

$$\mu_{ob}(E) = \ln(I_0/I), \tag{1}$$

where I_0 and I are incident and transmitted intensities of photons, respectively.

Figure 4 represents $\mu_{ob}(E)$ for $MnFeP_{0.56}Si_{0.44}$ at 25 K. Two x-ray absorption edges appear: one represents the Mn K absorption at 6539 eV; the other is the Fe K absorption at

7113 eV. There is a rather small energy separation between the Mn K edge and the following Fe K edge; that is, the range of the Mn K EXAFS is restricted between 6600 eV and 7100 eV. Here we will concentrate our discussion on EXAFS at the both Mn K and Fe K edge at 25 K, 100 K, 200 K, and 295 K. In order to obtain the EXAFS oscillation, a Victoreen's polynomial ($CE^3 + DE^4 + \text{const}$) was used to subtract the background signal. The background subtracted spectra are normalized at the energy of the absorption edge. We presume the absorption of an isolated Mn/Fe atom by using spline smoothing method. The EXAFS oscillation can be extracted from the absorption in this manner.

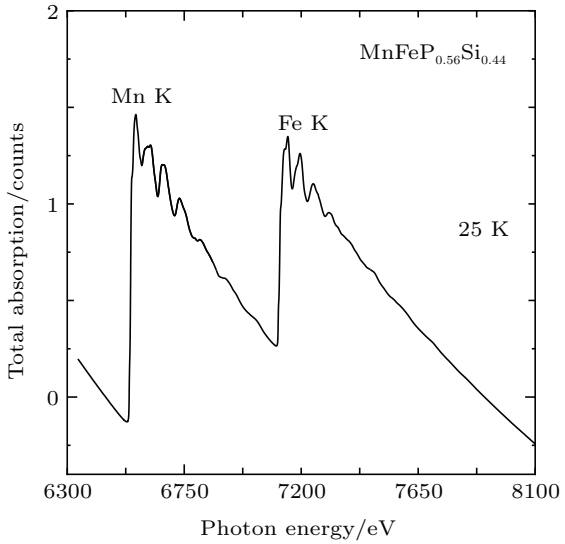


Fig. 4. The total x-ray absorption of $MnFeP_{0.56}Si_{0.44}$ against photon energy at 25 K.

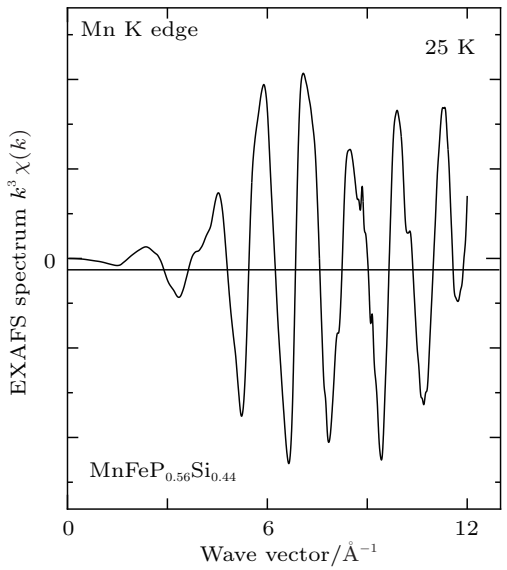


Fig. 5. EXAFS spectrum $k^3\chi(k)$ as a function of wave vector k for the Mn K edge at 25 K for $MnFeP_{0.56}Si_{0.44}$.

In Fig. 5, the weighted EXAFS oscillation $k^3\chi(k)$ of the Mn K edge for $MnFeP_{0.56}Si_{0.44}$ at 25 K is drawn as a function of the wave vector of photoelectron k. Fourier transformation of $k^3\chi(k)$ in the k space gives a radial structure function $\Phi(R)$ in the R space

$$\Phi(R) = \frac{1}{\sqrt{2\pi}} \int_{k_{\min}}^{k_{\max}} W(k) k^3 \chi(k) \exp(-2ikR)\,\mathrm{d}k, \quad (2)$$

where the interatomic distance R is the variable complementary to the wave vector k, $W(k)$ is the Hanning window function. We transform $k^3\chi(k)$ between 3.75 Å^{-1} and 11.95 Å^{-1} into $\Phi(R)$ for Mn K edge.

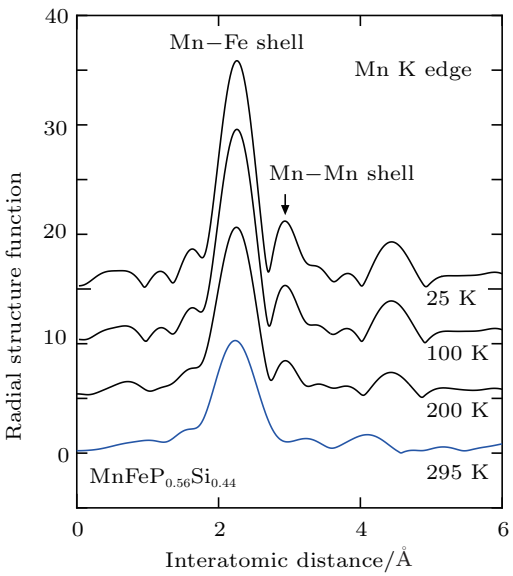


Fig. 6. (color online) The radial structure function of $MnFeP_{0.56}Si_{0.44}$ for the Mn K edge at 25 K, 100 K, 200 K, and 295 K.

The radial structure function $\Phi(R)$ is displayed in Fig. 6 for $MnFeP_{0.56}Si_{0.44}$ at 25 K, 100 K, 200 K, and 295 K. It should be noted that the distance in $\Phi(R)$ is shorter than the real one due to the phase shift. The peak at 2.27 Å corresponds to the first neighboring Mn–Fe pair along the c axis. On the other hand, the peak at 2.94 Å gives the second neighbor Mn–Mn distance in the c-plane. It can be seen that the peak position at 2.27 Å is almost independent of temperature. The peak at 2.94 Å is also independent of temperature 25 K to 200 K, while it disappears suddenly at 295 K. We suppose that its sudden change is related to the first-order magnetic transition at T_C. To determine the structural parameters, we convert $\Phi(R)$ into $k^3\chi(k)$ with the Fourier filtering technique; then, we fit the Fourier filtering $k^3\chi(k)$ spectrum to the following formula using the least-squares method,

$$k^3\chi(k) = \sum_i A_i(k) \sin[2kR_i + \delta_i(k)], \quad (3)$$

with the amplitude

$$A_i(k) = k^2 N_i |f_i(k,\pi)| \exp(-2(\sigma_i^2 k^2 + R_i/\lambda))/R_i^2. \quad (4)$$

Here, N_i is the coordination number, $f_i(k,\pi)$ is the backscattering amplitude, σ_i is the Debye–Waller factor, R_i is the interatomic distance between the absorbing and the i-th neighboring atom, δ_i is the phase shift and λ is the mean free path of

the photoelectron. We use the standard FEFF84 code[13,14] in EXAFS analysis to calculate the parameters such as $f_i(k, \pi)$ and δ_i based on the crystallographic parameters of Fe_2P-type structure. To reduce the number of disposable parameters in the fitting process, we set the restriction that the energy correction ΔE and the Debye–Waller factor have the same value for each shell.

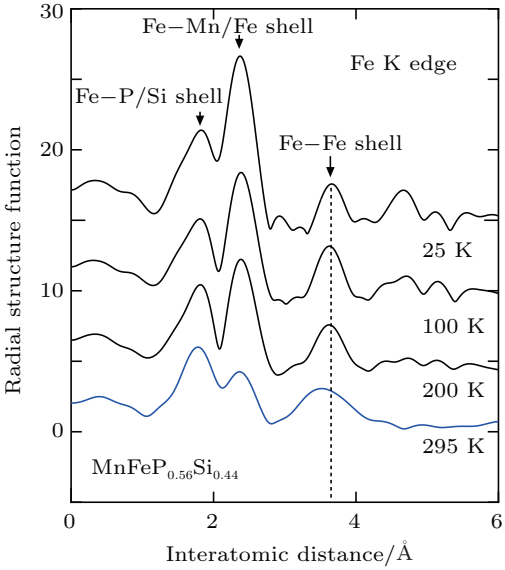


Fig. 7. (color online) The radial structure function of $MnFeP_{0.56}Si_{0.44}$ for the Fe K edge at 25 K, 100 K, 200 K, and 295 K.

Figure 7 shows the radial structure function of $MnFeP_{0.56}Si_{0.44}$ for Fe K edge at 25 K, 100 K, 200 K, and 295 K. The peak at shell (Fe–P/Si) of 1.77 Å indicates the P or Si atom in the neighborhood of Fe atom. The peak at 2.40 Å gives Fe–Mn and Fe–Fe pairs along the c axis and c-plane. On the other hand, the peak at 3.7 Å shows the second nearest neighbor atoms (Fe) around the Fe atom in c-plane. The peak positions at 1.77 Å and 2.40 Å are almost independent of temperature because the parameters a and c change with temperature in opposite sense.[10] The peak at 3.7 Å is also almost independent of temperature below 200 K, while it decreases at 295 K. As an example of analysis, figure 8 illustrates the Fourier-filtered spectrum of $MnFeP_{0.56}Si_{0.44}$ using the R range between 1.78 Å and 3.56 Å at the Mn K edge by open circles. The solid line shows the best fit of Eq. (2) to the spectrum, which is in good agreement with the spectrum.

According to the crystal symmetry of Fe_2P structure with the lattice parameters $a = b = 5.9823(0)$ Å and $c = 3.4551(1)$ Å, the Fe atom has four second nearest neighbors at 3.9632 Å if it is in the 3f site; it also has four second nearest neighbors at 3.1522 Å if it is in the 3g position. In Table 1 and Table 2 we tabulate the parameters of the local structure around the Mn and Fe atoms determined from the Mn K and Fe K edge EXAFS spectra of $MnFeP_{0.56}Si_{0.44}$ at 25 K, 100 K, 200 K, and 295 K. Our XAFS analysis shows that the Fe

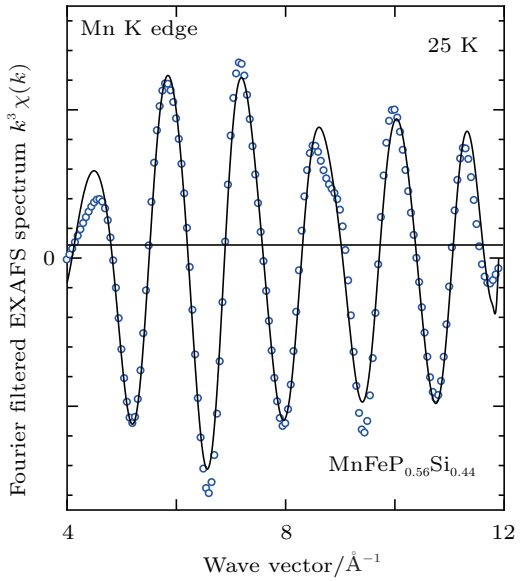


Fig. 8. (color online) Fourier filtered spectrum $k^3\chi(k)$ (open circle) plotted against wave vector k for $MnFeP_{0.56}Si_{0.44}$ at the Mn K edge. The solid line denotes the best fit.

atom has Fe neighbors at a distance of about 4.01 Å, which corresponds to the second nearest neighbor atoms around the Fe atom in the c-plane; the Mn atom possesses Mn pairs at about 3.22 Å, which correspond to the second nearest neighbor atoms around the Mn atoms in the c-plane at 25 K. All the 3g sites are occupied only by the Mn atoms, while the Fe atoms are located on the 3f sites and form an equilateral triangle. These new results are totally different from the previous neutron and x-ray diffraction results.[9,10] The interlayer distance between the 3f and 3g sites increases with increasing temperature. The Mn atoms at the 3g site have neighbors with a couple of Mn atoms along the c-plane and six Fe atoms at the 3f site along the c axis. For the 3g site in the c-plane, the Mn atom has two Mn atoms located at the distance of 3.22 Å as the second nearest neighbors at 25 K. The distance around the Mn atom in the 3g site is almost unchanged below 200 K and disappears at 295 K. The Fe atoms on the 3f site have six Mn atoms on the 3g site along the c axis. This interlayer distance between the 3f and 3g sites increases with increasing temperature. For the Fe–P/Si pairs, the nearest neighbor distance is independent of temperature, and the Debye–Waller factor increases as expected for a crystalline material with increasing temperature. In the 3f site on the c-plane the Fe atom has a pair of Fe atoms located at the distance of 2.65 Å as the first nearest neighbors and four Fe atoms at 4.01 Å as the second ones at 25 K. These distances around the Fe atom in the 3f site are constant within the error with increasing temperature from 25 K to 200 K, which decreases suddenly by nearly 2% for the first neighbors and by about 1% for the second ones at 295 K. Three Fe atoms at the 3f site and one Mn atom at the 3g site

form a tetrahedral structure. Based on the XAFS data, we calculated the volume of the tetrahedron in the ferromagnetic and the paramagnetic state. The estimated volume is 3.9823 Å^3 at 200 K (in the ferromagnetic phase) and 3.9937 Å^3 at 295 K (in the paramagnetic phase). When the material undergoes a transition from the ferromagnetic state to the paramagnetic state, the relative volume change is 2.8×10^{-3}, which is larger than the value of 0.64×10^{-3} for Fe_2P reported by Fujii *et al.*[8] EXAFS provides the local atomic structure for a selected atomic species, while XRD provides information about the unit cell dimensions, which comes from the average effect of the overall crystal. Therefore, it is reasonable to presume that the local structure of the Fe in this material is greatly distorted, which probably results from magnetoelastic coupling. Delczeg-Czirjak *et al.* pointed out that in the MnFePSi compound, stabilization of the ferromagnetic structure is due to the localization of the Fe moments induced by the larger Fe–Fe distance in the ferromagnetic phase.[15] Our results show that the Fe–Fe distance change between the ferromagnetic and the paramagnetic states is up to 2% in the $MnFeP_{0.56}Si_{0.44}$ compound. We presume that this large change comes from the magnetoelastic effect and plays an important role in determining the first-order phase transition. The distance between the 3g and 3f layers, derived from the Mn K edge, is shorter than that derived from the Fe K edge. The accuracy of the derived structural parameters for the Mn K edge is somewhat lower than that of the Fe K edge due to the limited energy range. On the other hand, this may be affected by the distortion of the local environment of the Fe atoms, because the distances between the Fe atom and its first nearest neighbor atoms in the 3f-layer are similar to the distance between the 3g and 3f layers.

Table 1. Structural parameters of $MnFeP_{0.56}Si_{0.44}$ determined from the Mn K edge EXAFS at temperatures 25 K, 100 K, 200 K, and 295 K, where A is an absorbing atom, B is a backscattering atom, N is the coordination number, R is the interatomic distance, σ is the Debye–Waller factor, and ΔE is the threshold energy difference. The fitting parameters are N, R, σ, and ΔE.

A–B pairs	Temperature/K	N	R/ Å	ΔE/eV	σ/Å
Mn(3g)–Fe(3f)	25	5.73(1.0)	2.66(0.01)	0.56(0.01)	0.07(0.02)
	100	5.74(1.0)	2.66(0.01)	0.79(0.01)	0.08(0.01)
	200	5.76(1.0)	2.66(0.01)	1.13(0.02)	0.09(0.01)
	295	5.52(1.0)	2.68(0.01)	0.13(0.01)	0.10(0.01)
Mn(3g)–Mn(3g)	25	1.70(1.0)	3.22(0.01)	0.56(0.01)	0.07(0.02)
	100	1.55(1.0)	3.22(0.01)	0.79(0.01)	0.08(0.01)
	200	1.35(1.0)	3.21(0.02)	1.13(0.02)	0.09(0.01)
	295	–	–	–	–

Table 2. Structural parameters of $MnFeP_{0.56}Si_{0.44}$ determined from the Fe K edge EXAFS at temperatures 25 K, 100 K, 200 K, and 295 K, where A is an absorbing atom, B is a backscattering atom, N is the coordination number, R is the interatomic distance, σ is the Debye–Waller factor, and ΔE is the threshold energy difference. The fitting parameters are N, R, σ, and ΔE.

A–B pairs	Temperature/K	N	R/Å	ΔE/eV	σ/Å
Fe(3f)–Mn/(3g)	25	5.57(1.0)	2.73(0.01)	3.77(0.01)	0.09(0.01)
	100	5.46(1.0)	2.74(0.01)	4.54(0.01)	0.10(0.01)
	200	5.23(1.0)	2.74(0.01)	3.03(0.01)	0.11(0.01)
	295	5.09(1.0)	2.75(0.02))	0.69(0.01)	0.12(0.01)
Fe(3f)–Fe/(3f)	25	1.95(1.0)	2.65(0.01)	3.77(0.01)	0.09(0.01)
	100	1.85(1.0)	2.66(0.01)	4.54(0.01)	0.10(0.01)
	200	1.80(1.0)	2.65(0.01)	3.03(0.02)	0.11(0.01)
	295	1.74(1.0)	2.61(0.01)	0.69(0.01)	0.12(0.02)
Fe(3f)–Fe/(3f)	25	4.00(1.0)	4.01(0.00)	3.77(0.01)	0.09(0.01)
	100	4.04(1.0)	4.01(0.01)	4.54(0.00)	0.10(0.01)
	200	4.95(1.0)	4.00(0.02)	3.03(0.02)	0.11(0.01)
	295	4.05(1.0)	3.96(0.02)	0.69(0.01)	0.12(0.01)
Fe(3f)–P(1b/2c)	25	1.95(1.0)	2.28(0.01)	3.77(0.01)	0.09(0.01)
	100	1.87(1.0)	2.28(0.01)	4.54(0.01)	0.10(0.01)
	200	2.04(1.0)	2.28(0.01)	3.03(0.01)	0.11(0.02)
	295	1.76(1.0)	2.28(0.01)	0.69(0.01)	0.12(0.01)
Fe(3f)–Si(1b/2c)	25	1.95(1.0)	2.27(0.01)	3.77(0.01)	0.09(0.01)
	100	1.82(1.0)	2.25(0.01)	4.54(0.01)	0.10(0.01)
	200	1.74(1.0)	2.27(0.01)	3.03(0.02)	0.11(0.02)
	295	2.05(1.0)	2.28(0.01)	0.69(0.00)	0.12(0.04)

4. Conclusion

In conclusion, the local structures around the Fe atoms and the Mn atoms in the $MnFeP_{0.56}Si_{0.44}$ compound have been determined from the Fe K and Mn K edge EXAFS spectra. The Fe and Mn atoms occupy the 3f and 3g sites, respectively. This is a new observation, differing from previous reports. In 3f layers the first and the second Fe–Fe neighboring distances exhibit large changes at the magnetic transition. These large changes come from the magnetoelastic effect and play an important role in determining the first-order phase transition.

References

[1] Brück E 2005 *J. Phys. D: Appl. Phys.* **38** R381

[2] Tegus O, Brück E, Buschow K H J and de Boer F R 2002 *Nature* **415** 150

[3] Pecharsky V K and Gschneidner K A Jr 1997 *Phys. Rev. Lett.* **78** 4494

[4] Pecharsky V K and Gschneidner K A Jr 1997 *J. Magn. Magn. Mater.* **167** L179

[5] Wada H and Tanabe Y 2001 *Appl. Phys. Lett.* **79** 3302

[6] Dagula W, Tegus O, Fuquan B, Zhang L, Si P Z, Zhang M, Zhang W S, Brück E, de Boer F R and Buschow K H J 2005 *IEEE Trans. Magn.* **41** 2778

[7] Geng Y X, Tegus O and Bilige Q 2012 *Chin. Phys. B* **21** 037504

[8] Fujii H, Hōkabe T, Kamigaichi T and Okamoto T 1977 *J. Phys. Soc. Jpn.* **43** 41

[9] Zhang L, Moze O, Prokes K, Tegus O and Brück E 2005 *J. Magn. Magn. Mater.* **290** 679

[10] Höglin V, Hudl M, Sahlberg M, Nordblad P, Beran P and Andersson Y 2011 *J. Solid State Chem.* **184** 2434

[11] Li Y J, Huliyageqi B, Haschaolu W, Song Z Q, Tegus O and Nakai Ikuo 2014 *J. Electron Spectrosc. Relat.* **196** 104

[12] Nomura M and Koyama A 1996 *BL-12C, KEK Report* **95** 15

[13] Ankudinov A L, Nesvizhskii A I and Rehr J J 2003 *Phys. Rev. B* **67** 115120

[14] Rehr J J, Mustre de Leon J, Zabinsky S I and Albers R C 1991 *J. Am. Chem. Soc.* **113** 5135

[15] Delczeg-Czirjak E K, Pereiro M, Bergqvist L, Kvashnin Y O, Di Marco I, Guijiang Li, Vitos L and Eriksson O 2014 *Phys. Rev. B* **90** 214436